Sains Malaysiana 43(2)(2014): 261–265

Using a Pilot Plant to Synthesise ZnO Powder: Particle Characterisation and Marine Toxicity Studies

(Menggunakan Loji Pandu untuk Mensintesis Serbuk ZnO: Pencirian Partikel dan Kajian Ketoksikan Marin)

S. MAHMUD* & Z. DIN

ABSTRACT

A zinc oxide (ZnO) pilot plant furnace was used to synthesize ZnO nanoparticles at very high capacities in a range of 1-4 t/month. The 4-t custom-designed furnace was used to synthesize ZnO particles possessing primary nanoparticles resembling rods and grains. At a combustion temperature of 1000-1300°C, zinc vapour was oxidized into ZnO powder in order to produce granular ZnO (ZG) particles. By blowing air into the combustion chamber, ZnO nanorods (ZR) were produced. The ZR specimen exhibited higher XRD intensities, stronger photocatalysis and higher electrical resistance compared to that of ZG sample. However, the ZR sample showed a stronger toxicity to marine phytoplankton, Isochrysis galbana*, by starting to inhibit cell growth at 8 mg/L ZnO concentration in seawater whereas ZG sample started showing growth inhibition at a higher ZnO concentration of 32 mg/L. The toxicity of ZnO primary nanoparticles was probably attributed to the dissolution, release and uptake of free zinc ions especially for the case of the higher surface area of ZR particles that exhibited relatively higher zinc concentration on the particle surface, based on the elemental mapping of the electron spectroscopy imaging results.*

Keywords: Isochrysis galbana*; pilot plant; toxicity; ZnO*

ABSTRAK

Satu tanur loji pandu zink oksida (ZnO) digunakan untuk menghasilkan partikel nano ZnO pada kapasiti tinggi dalam julat 1-4 t/bulan. Dengan reka bentuk-khusus, tanur seberat 4 t ini digunakan untuk mensintesis partikel ZnO yang memiliki partikel nano primer menyerupai rod dan butiran. Pada suhu pembakaran 1000-1300°C, wap zink dioksidakan menjadi ZnO untuk menghasilkan partikel butiran ZnO (ZG). Dengan meniup udara ke dalam kebuk pembakaran, nanorod ZnO (ZR) dihasilkan. Sampel ZR mempamerkan keamatan XRD yang lebih tinggi, fotokatalisis yang lebih kuat dan kerintangan elektrik yang lebih tinggi jika dibandingkan dengan ciri sampel ZG. Walau bagaimanapun, sampel ZR menunjukkan ketoksikan yang lebih kuat terhadap fitoplankton marin, Isochrysis galbana *dengan merencat pertumbuhan sel pada kepekatan 8 mg/L ZnO dalam air laut manakala sampel ZG menunjukkan rencatan pertumbuhan sel pada kepekatan 32 mg/L. Ketoksikan partikel nano primer ZnO mungkin disebabkan oleh pelarutan, pembebasan dan pengambilan ion bebas zink terutama untuk kes partikel ZR yang memiliki keluasan permukaan yang lebih tinggi dan kepekatan zink relatif yang lebih tinggi di permukaan partikel, berdasarkan kepada data pemetaan unsur daripada maklumat pengimejan elektron spektroskopi.*

Kata kunci: Isochrysis galbana*; ketoksikan; loji pandu; ZnO*

INTRODUCTION

Zinc oxide (ZnO) is a versatile material that finds applications in industries relating to rubber, ceramics, catalysis, sunscreen, baby powder, varistors, ferrites, coatings, animal feed and many biomedical uses (Mahmud 2011; Moezzi et al. 2012; Shi et al. 2011). ZnO is a popular II-VI semiconductor possessing a hexagonal wurtzite structure with a direct energy bandgap of 3.37 eV at room temperature combined with a strong and characteristic ultraviolet (UV) luminescence at 360-395 nm (Shi et al. 2011). Potential applications of ZnO include industries related to liquid crystal display, light emitting diodes, spintronics, nano solar cells, nano medicine, sensors and nano textiles (Moezzi et al. 2012).

In this paper, we report an effort to produce zinc oxide (ZnO) nanoparticles in tonnage capacities using a custom-designed pilot plant foundry that is capable of synthesizing ZnO particles with rod-like and granular morphologies at capacities exceeding one t/month. The motivation of this work was to investigate the capabilities of the ZnO foundry in producing ZnO particles with selective morphology. Another objective was to study the structural, optoelectronic and toxicity properties of the ZnO morphologies in order to observe interesting morphology-induced responses. High aspect ratio morphologies (such as rods and wires) tend to possess stronger physical reactivity, excellent photocatalysis and higher electrical resistivity if compared to that of morphologies with lower aspect ratios

(such as spheroids and grains) (Mahmud 2011; Moezzi et al. 2012; Shi et al. 2011). Little work has been reported on the marine toxicity of ZnO particles possessing different shapes and sizes. Many workers proposed the dissolution, release and uptake of free zinc ions as the underlying cause of toxicity whereby the level of toxicity can be determined by the shape and size of ZnO particles (Nafchi et al. 2012; Wagner et al. 2011).

Materials and Methods

We designed and built an electric-powered ZnO pilot plant foundry consisted of a zinc boiling furnace, cooling pipe system and a bag house giving a total weight of about 4 t. Figure 1(a) shows the cross-section diagram of the furnace with key internal parts that include a graphite crucible (70 kg maximum loading), refractories with embedded heating elements and a thermocouple system for autonomous temperature control. Graphite crucible was used due to its excellent chemical and physical stability during high temperature process. Furnace linings are made of heavy-duty refractory castables with embedded 16 kW kanthal heating elements capable of heating up to 1400ºC. After charging the furnace with zinc ingots (Zinifex 99.995% zinc content), the electric heater was switched on in order to raise the furnace temperature above the boiling point of zinc (907ºC) resulting in the release of zinc vapour that instantly oxidized into ZnO powder that squeezed through the steel cover orifice to escape the furnace. The oxidation process had a combustion-like appearance with strong white luminescence. Safety measures such as wearing fire-resistant apparels (gloves, suit and hood) were taken during the experiment due to hazardous open flame radiation. To selectively make ZnO particles of a certain morphology and size, the furnace temperature was varied from 1000 to 1300ºC whereby granular morphology was produced with temperature set at 1200-1300ºC. For the synthesis of nanorods, air was supplied into the combustion area (above steel cover) and the furnace temperature was reduced to 1100-1200ºC. Freshly oxidized powder was sucked into a piping system designed for rapid cooling of the hot powder. Finally the ZnO powder was collected by the filter bags in the baghouse.

In this paper, ZnO grain is abbreviated as ZG while ZnO nanorods as ZR. The as-grown ZG and ZR particles were analyzed with a LEOSupra50VP field emission scanning electron microscope (FESEM) equipped with energy dispersive spectrometry (EDS), a Panalytical X'pert Pro Mrd Pw3040 x-ray diffractometer with Cu K_α radiation (λ=1.5406Å) excitation, a Zeiss Libra-120 energy filter transmission electron microscope (EFTEM) equipped with electron spectroscopy imaging (EFTEM-ESI) for elemental mapping, a Phillip CM12 transmission electron microscope (TEM) and a Jobin Yvon Horiba HR800UV photoluminescent (PL) spectroscopy unit with 325 nm excitation source (from HeCd laser). A novel non-destructive method was employed for electrical resistance measurement as described in our previous work (Mahmud 2011). Electrical measurement was performed using a Keithly 251 (model 82-138) I-V tester.

For toxicity test, a marine phytoplankton, *I. galbana*, was chosen due to its abundance in Malaysian ocean coastline. The phytoplankton strain, obtained from the Institute of Fisheries Research Pulau Pinang, was grown in seawater enriched by Conway solution. After soaking all flasks in 5% concentrated H_2SO_4 and rinsing in double distilled water, the flasks and seawater were autoclaved at 123ºC and 15 psi for 20 min. The cells were grown in Conway medium whereby the pH of the culture was observed at 8.5, salinity at 25 ppt and temperature of 23.4ºC. After agitating at 150 rpm, the test solutions were exposed to a fluorescent white light with a light intensity of 20-25 μmol/m^2/s. A range of nominal ZnO concentrations (mg/L) of the test seawater were prepared (0, 8, 16, 32, 64, 128 mg/L) from standard solution. Daily measurement of cell concentration was performed using an improved Neubauer haemacytometer at 10 times magnification under an optical microscope. The calculation method of algal cells was in accordance to a procedure described by Martinez et al. (1975).

Results and Discussion

Figure 1(a) shows a cross-section of the custom-built furnace that is made up of a graphite crucible, castable refractories with embedded heating elements, steel cover with a central orifice and thermocouple for temperature control. ZnO particles with various morphologies such as ZnO nanorods (Figure 1(b)) can be easily produced at high capacity exceeding one t/month. Furnace temperature played a dominant role in determining the output capacity whereby the capacity can be increased from 1.08 t/month (1.5 kg/h) at 1000ºC furnace temperature to 5.6 t/month (4.0 kg/h) at 1300ºC furnace temperature as shown in Figure 1(c). A photograph of the ZnO plant is posted in Figure 2(a) that shows the cooling pipe, suction hood, heat exchanger and bag house whereby Figure 2(b) shows the furnace in operation. Combustion flame was evident during zinc oxidation process. The intense white luminescence was a by-product of zinc oxidation. Since the furnace is powered by electricity, no combustion gas was released to the environment. The powder filtering of the bag house was also excellent whereby no powder was seen to escape through the exhaust pipe. The cooling pipe system was equipped with a heat exchanger that produced clean hot air that can be channelled to other applications such as drying wet laundry. In a nut shell, the plant design is green, environmental friendly and sustainable. Even though using electricity can raise the production cost by 30-40%, the pilot plant is capable of selectively synthesize ZnO with specific morphology (in nano size).

A probable growth mechanism is proposed for the exciting synthesis as illustrated in Figure 1(a). Above 907ºC, zinc boils to produce zinc vapour. The high supersaturation state in the crucible leads to the formation of ZnO nuclei particles that nucleate from the gas phase.

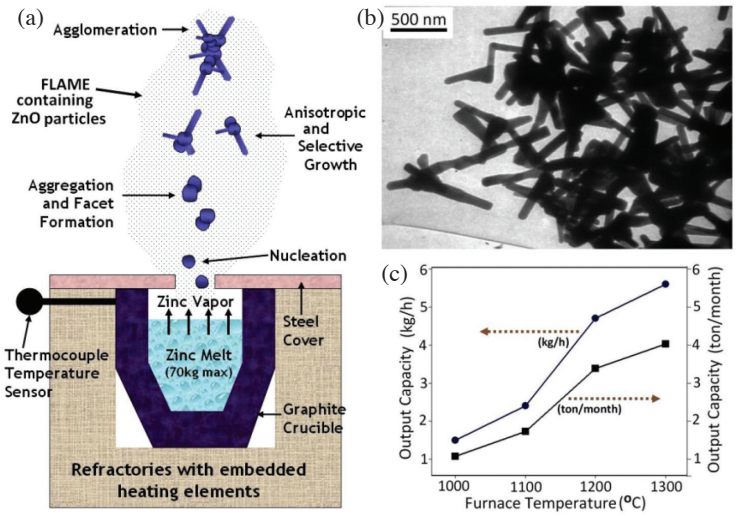

FIGURE 1. (a) Schematic diagram of the foundry furnace showing a probable growth mechanism, (b) TEM micrograph of high-density ZnO nanorods produced by the pilot plant and (c) output capacity of the plant with respect to furnace temperature

These particles coagulate to form aggregates with crystal facets that serve as the 'nucleating planes' for subsequent anisotropic growth (Mahmud 2011). The selective growth of a certain morphology depends on the crystal facets such as (0002), (10 $\bar{1}$ 0), (10 $\bar{1}$ 1) and (11 $\bar{2}$ 0). Rods with a hexagonal cross-section would require (0002) nucleating planes whereby rods with rectangular cross-section would require (10 $\bar{1}$ 0) or (11 $\bar{2}$ 0) nucleating planes. Anisotropic growth will take place as more Zn-O bonds attach on the aggregates. An aggregate may consists of several primary particles and primary particles may resemble rods, wires, drums, plates and boxes. Micron size agglomerates are produced as aggregates coalesce by forming sintered bridges at contact surfaces. An example of an aggregate agglomeration is posted in the TEM micrograph of Figure 1(b) whereby the primary particles are ZnO nanorods with 50-90 nm width and 200-700 nm length. An aggregate may consists of 2-8 nanorods and several aggregates coalesced to form the larger agglomerate.

For this work, two common ZnO morphologies were investigated namely nanorods (ZR) and grains (ZG) that were observed to have whitish appearance. Typical ZR particles are posted in the TEM micrograph of Figure 2(c) that show ZnO nanorods with 40-90 nm width and 100-250 nm length whereby ZG particles are posted in the TEM micrograph of Figure 2(d) that show grain-like shape with dimensions of 120-300 nm. The XRD spectra in Figure 2(e) shows many diffraction peaks for both samples thereby confirming that the as-grown ZnO particles are polycrystalline in nature. By comparing the diffraction peaks of JCPDS card 36-1451 (for ZnO structure) with the diffraction peaks of Figure 2(e) at 32.1° (10 $\bar{1}$ 0), 34.2° (0002), 36.3° (10 $\bar{1}$ 1), 47.5° (10 $\bar{1}$ 2) and 56.5° (11 $\bar{2}$ 0), it can be concluded that the ZR and ZG powder possess wurtzite ZnO structure. The intense and narrow XRD diffraction peaks of (10 $\bar{1}$ 0), (0002) and (10 $\bar{1}$ 1) suggest a high level of crystallinity of the as-grown powder. The relatively higher XRD peak intensities of ZR sample, especially (10 $\bar{1}$ 1) peak at 1580 a.u., compared to that of ZG sample (only 820 a.u. for (10 $\bar{1}$ 1) peak) indicate the superior crystallinity of ZR particles. The ZR superior polycrystals can be attributed to the higher partial oxygen pressure coming from the air supply during zinc oxidation process in that the extra oxygen could have enhanced the formation of stable hexagonal wurtzite structure of ZnO.

The superior ZR crystallinity is also supported by the relatively higher PL intensity of ZR particles (about 5000 a.u.) at the UV band edge of 384 nm as posted in Figure 2(f) if compared to the PL intensity of ZG particles (about 350 a.u.) at 382 nm. The UV band edge emission at 382/384 nm was attributed to the near band edge transition of ZnO relating to the recombination of the free excitons. From the PL emission spectra, it can also be concluded that ZR particles possess a much higher photo-catalysis than ZG particles. An interesting PL emission can be seen at 765 nm (red-infrared region) for ZR sample where Karali et al. (2005) attributed this red-infrared emission to the presence of free zinc in the sample. The presence of free zinc on ZnO powder is a real industrial problem faced by ZnO manufacturers and this problem can be attributed by incomplete oxidation due to rapid quenching induced by air supply to the combustion area; however, the real cause is still unclear.

For electrical measurement, pellets were prepared from the ZR and ZG powder in accordance to the non-destructive method described in our previous work (Mahmud 2011) and the surface resistance is reported in Figure 2(g). The measurement was done by current-triggering to give the V-I curves; it was found current-triggering gave a more stable response if compared to voltage-triggering approach. From Figure 2(g), it is clear that the ZR specimen exhibited a much higher surface

resistance (0.622 GΩ) than the surface resistance of ZG sample (0.0517 GΩ). Giga-ohm resistance values are common for undoped or pure ZnO. The large surface resistance of ZR sample (twelve times bigger than that of ZG sample) can be attributed to the intrinsic defects on the surface of the nanorods whereby the surface intrinsic defects served as charge trappers that reduced current flow. A probable intrinsic defect on the nanorod surface is free zinc or interstitial zinc as indicated by the red-infrared PL emission in Figure 2(f). Another supporting data for the free-zinc theory is provided by the elemental mapping of EFTEM-ESI results posted in Figure 3. We were fortunate to obtain a ZnO nanorod resting next to a ZnO grain because this allowed us to perform oxygen and zinc mapping simultaneously for both morphologies. By comparing the oxygen and zinc maps of Figure 3(b) and 3(c), it is evident that the ZnO nanorod possessed much more zinc elements on the surface if compared to the oxygen elements. An opposite trend is observed for the ZnO grain where the zinc on the surface appeared to be less than oxygen; in other words, ZnO grains tend to have more oxygen elements than zinc elements on the surface. It can also be postulated that the method of particle synthesis during zinc oxidation played a major role in controlling the zinc-to-oxygen ratio on the particle surface and a high zinc-to-oxygen ratio case (as per ZR nanorod case) can result in large intrinsic Zn^{2+} defects that can trap charges during electrical measurement.

Figure 4 shows the toxicity results of ZR and ZG particles on marine phytoplankton *I. galbana* and a FESEM micrograph of the *I. galbana* is shown in the inset of Figure 4(c). From Figure 4(a), inhibition of cell growth appeared to start at 8 mg/L for ZR sample after 4 days and for ZG sample, growth inhibition seemed to begin at a higher concentration of 32 mg/L in seawater (Figure 4(b)). The 4-day EC_{50} value is 19.05 mg/L for ZR sample indicating that it took 19.05 mg/L of ZnO concentration to reduce population growth by half (Figure 4(c)). The EC_{50} value for ZG sample was higher (at 32.85 mg/L) meaning that more ZnO grains were needed to halve population growth after 4 days. It can be concluded that the nanorods in ZR sample exhibited a stronger toxicity on marine phytoplankton *I. galbana*. The higher ZR toxicity on *I. galbana* can be attributed to the larger nanorod surface area that enhanced zinc dissolution into seawater. Moreover, the larger zinc-to-oxygen ratio of ZR particles (based on the elemental maps of Figure 3) could also provide more zinc supply for dissolution into seawater bath. Probable explanation for the cell growth inhibition could be due to the zinc presence (in seawater bath) that disturbed cell division and

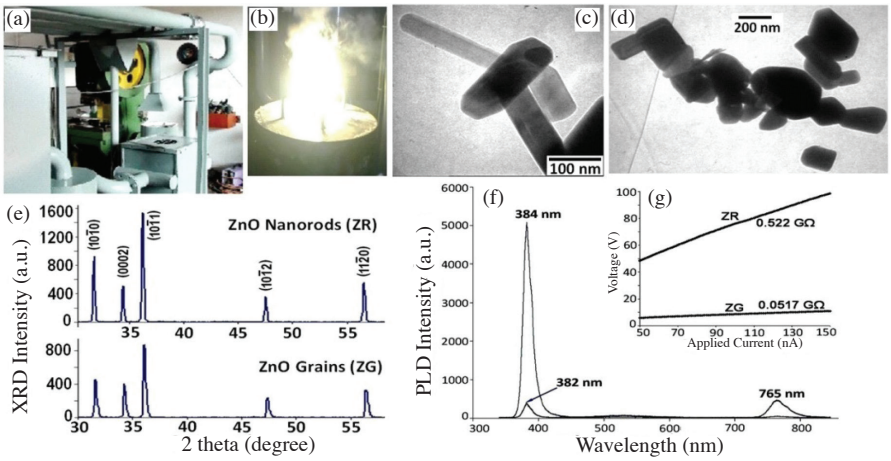

FIGURE 2. (a) Photographs of the 4-t ZnO foundry, (b) combustion flame during zinc oxidation, (c) TEM micrographs of as-grown ZnO nanorods, (d) as-grown ZnO grains, (e) XRD data of ZR and ZG samples, (f) PL spectra and (g) electrical response of both samples

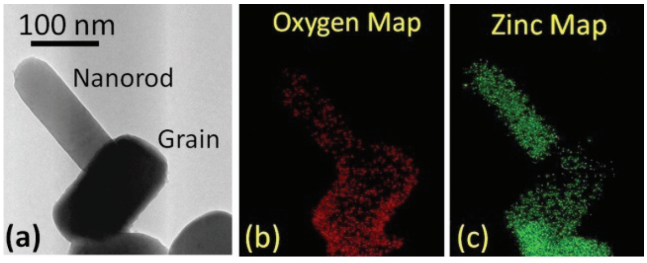

FIGURE 3. EFTEM-ESI data showing (a) EFTEM micrograph of a ZnO nanorod (ZR) conveniently resting next to a ZnO grain (ZG) and the corresponding elemental mapping for (b) oxygen and (c) zinc atoms

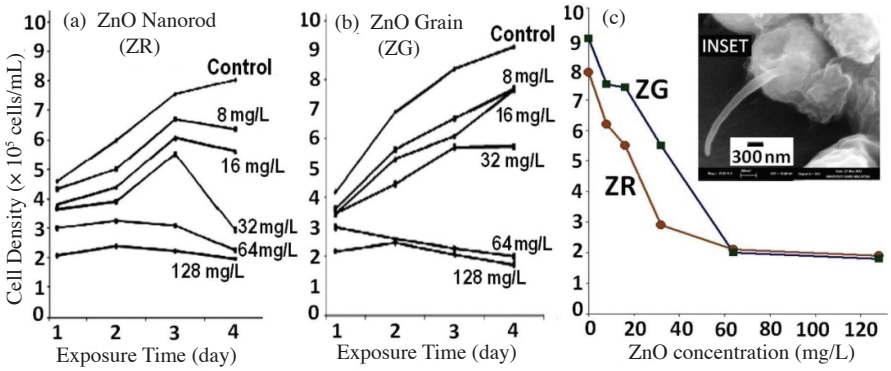

FIGURE 4. Toxicity results showing cell density data for (a) ZR sample, (b) ZG samples and (c) relative E_{50} determination (FESEM micrograph of *I. galbana* in INSET)

photosynthetic mechanism of the alga (Overnell 1975). The permeability of the cell membrane could also be disrupted by the zinc presence causing K^+ loss and volume changes of the cell.

CONCLUSION

We report the building and usage of a high-capacity machine capable of producing ZnO particles with granular and nanorod morphologies in tonnage capacities. The ZnO nanorods tend to possess larger surface area and zinc concentration (on the surface) that may be the underlying causes for the larger electrical resistance, stronger UV photocatalysis and higher toxicity on marine phytoplanktons.

ACKNOWLEDGMENTS

This work is supported by a short term grant (304/PFIZIK/6312077) from Universiti Sains Malaysia. We also acknowledged the assistance from Lailawati Hazwani Saad, Nazurah Hanim Mamat and Ng Bee Wah.

REFERENCES

Karali, T., Can, N., Valberg, L., Stephanov, A.L., Townsend, P.D., Bucha, Ch., Ganeev, R.A., Ryasnyansky, A.I., Belik, H.G., Jessett, M.L. & Ong, C. 2005. Optical properties and luminescence of metallic nanoclusters in ZnO:Cu. *Physica B: Condensed Matter* 363: 88-95.

Mahmud, S. 2011. One-dimensional growth of zinc oxide nanostructures from large micro-particles in a highly rapid synthesis. *Journal of Alloys and Compounds* 509(9): 4035-4040.

Martinez, M.P., Chakroff, J.B. & Pantastica, J.B. 1975. Direct phytoplankton counting technique using the hemacytometer. *Philippine Agricultural Scientist* 59: 43-50.

Moezzi, A., McDonagh, A.M. & Cortie, M.B. 2012. Zinc oxide particles: Synthesis, properties and applications. *Chemical Engineering Journal* 185-186: 1-22.

Nafchi, A.M., Alias, A.K., Mahmud, S. & Robal, M. 2012. Antimicrobial, rheological, and physicochemical properties of sago starch films filled with nanorod-rich zinc oxide. *Journal of Food Engineering* 113(4): 511-519.

Overnell, J. 1975. The effect of heavy metals on photosynthesis and loss of cell potassium in two species of marine algae. *Marine Biology* 29: 99-103.

Shi, J., Hong, J.H., Ding, Y., Yang, Y., Wang, F., Cai, W. & Wang, X. 2011. Evolution of zinc oxide nanostructures through kinetics control. *Journal of Materials Chemistry* 21: 9000-9008.

Wagner, S., Bloh, J., Kasper, C. & Bahnemann, D. 2011. Toxicological issues of nanoparticles employed in photocatalysis. *The Green Journal* 1(2): 171-188.

Shahrom Mahmud*
Zinc Oxide Research & Innovation (ZORI) Team
Nano-Optoelectronic Research Lab
School of Physics, Universiti Sains Malaysia
11800 Pulau Pinang
Malaysia

Shahrom Mahmud*
Academy of Sciences Malaysia
902-4 Jalan Tun Ismail
50480 Kuala Lumpur
Malaysia

Zubir Din
Marine Pollution and Toxicology Unit
School of Biological Sciences, Universiti Sains Malaysia
11800 Pulau Pinang
Malaysia

*Corresponding author; email: shahromx@usm.my

Received: 7 January 2013
Accepted: 19 July 2013